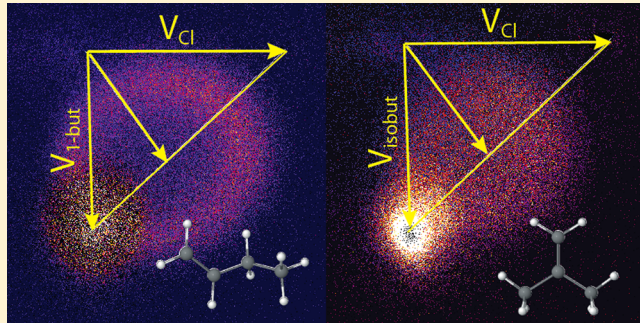


Crossed-Beam Slice Imaging of Cl Reaction Dynamics with Butene Isomers

Baptiste Joalland, Richard Van Camp, Yuanyuan Shi, Nitin Patel, and Arthur G. Suits*

Department of Chemistry, Wayne State University, Detroit, Michigan 48202, United States

ABSTRACT: We present a crossed-beam imaging study of the reaction of chlorine atoms with several butene isomers. A high-intensity pulsed ablation Cl source is used with DC slice imaging and single-photon ionization detection at 157 nm to record the velocity-flux contour maps for these reactions. The target unsaturated hydrocarbons are 1-butene, *trans*-2-butene, *cis*-2-butene, and isobutene (2-methylpropene). Data are obtained at collision energies of $\sim 13.0 \text{ kcal}\cdot\text{mol}^{-1}$. Distinct differences in the scattering distributions and in particular the coupling of angular and translational energy release provide insight into the dynamics of this little-studied class of reactions. We find that these distributions reflect the energetics for competition between addition/elimination and direct abstraction in line with ab initio thermochemical data. A possible role for Cl atom roaming mediating the addition/elimination pathway is suggested.



I. INTRODUCTION

Reactions of chlorine atoms with hydrocarbons have become an important benchmark in the study of polyatomic reaction dynamics.¹ This is because these reactions are relatively fast, barrierless, or nearly so, and because they afford the opportunity to explore distinct dynamics for different reactive sites^{2–5} and isomers, or to examine the influence of initial vibrational excitation^{6–8} on the dynamics. Dynamical studies have ranged from state-resolved PHOTOLOC studies,^{9,10} to crossed-beam imaging with both universal^{11,12} and state-resolved detection,¹³ to PHOTOLOC imaging¹⁴ augmented by dynamical calculations. All of these studies have been interpreted with various simple models of the dynamics.

Although extensively investigated for their kinetics,^{15,16} reactions of Cl atoms with alkenes have been much less frequently reported in dynamical studies, yet they provide a fascinating opportunity to explore the influence of large variations in exoergicity for different target sites, and the possible influence of a strongly bound adduct ($\sim 1 \text{ eV}$) mediating the dynamics under some conditions. We recently reported a crossed-beam study of Cl reactions with 1-pentene and a number of hexene isomers at 4 and $7 \text{ kcal}\cdot\text{mol}^{-1}$ collision energies.¹⁷ The chief findings in that study were that the reactions were dominated by complex formation at low collision energy while the high collision energy reactions began to show evidence of a stripping mechanism in the forward direction ascribed to direct abstraction of the alkylic H atom sites.

In the present work, we focus on the reaction dynamics for atomic chlorine with a series of butene isomers shown in Figure 1, with energetics referred to the reactants. The H abstraction and addition energetics have been calculated at the CBS-QB3 level of theory.^{18,19} In all cases, Cl addition to the double bond

contributes about $20 \text{ kcal}\cdot\text{mol}^{-1}$ stabilization energy, with reaction at remote alkylic sites exoergic by $3\text{--}4 \text{ kcal}\cdot\text{mol}^{-1}$, reaction at vinylic sites endoergic by $3\text{--}5 \text{ kcal}\cdot\text{mol}^{-1}$, and reaction at allylic sites exoergic by $15\text{--}20 \text{ kcal}\cdot\text{mol}^{-1}$. These are largely consistent with those we reported earlier for 1-pentene.

II. EXPERIMENTAL SECTION

The experiments were conducted in a crossed-beam imaging apparatus described in detail previously.^{12,20,21} These studies made use of a high density Cl atom source that relies on a plasma generated by impact of 20 mJ pulses at 355 nm onto an aluminum tube of $\sim 2 \text{ mm}$ inner diameter, while a pulse of 3% Cl_2 in helium is passed through. The result is an intense Cl beam at $\sim 1700 \text{ m/s}$ with a speed ratio of ~ 10 . We find the intensity at least an order of magnitude larger than our previous approaches relying on 193 nm photolysis of oxalyl chloride at the (unconfined) tip of the nozzle.^{12,20} The distance from the nozzle to the skimmer is approximately 75 mm , and from the skimmer to the subsequent interaction region, another 75 mm . The 355 nm beam was focused by a 350 mm focal length lens and introduced to the source chamber through the main chamber via an isolated tube, which is connected to the source region with Cajon fittings. This is essentially the same configuration we have used for many scattering experiments with the exception, mentioned above, of the introduction of a tubular aluminum extension on the pulsed valve nozzle with an inner diameter slightly larger than the nozzle opening itself. A

Special Issue: Joel M. Bowman Festschrift

Received: March 27, 2013

Revised: May 29, 2013

Published: May 30, 2013

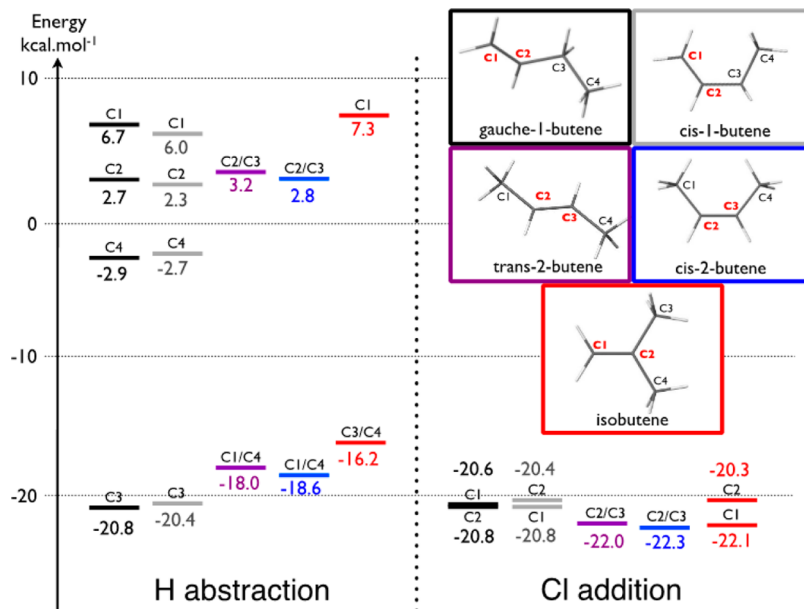


Figure 1. Energy diagram for Cl reactions with gauche-1-butene (black), cis-1-butene (gray), cis-2-butene (blue), trans-2-butene (purple), and isobutene (red), calculated at the CBS-QB3 level of theory. Unsaturated carbons are highlighted in red on the structures. On the left are reaction enthalpies (0 K) for H abstraction at the indicated sites. On the right are energy minima for Cl addition.

narrow port allows access of the 355 nm pulse very close to the nozzle opening, and the pulse strikes the wall of the aluminum tube creating an ablation plasma that increases the density of free Cl atoms significantly. The butene beams were produced by seeding the appropriate isomer at ~3% in helium. Stagnation pressures in both beams were ~5 bar, and both beams were generated with piezoelectric disk based valves set for a pulse duration of 100 μ s.

The probe laser was a fluorine excimer (GAM EX-10) operating at 10 Hz, generating a VUV beam at 157 nm. The beam path was purged with dry nitrogen, and the laser was unfocused. Power was attenuated to ~0.5 mJ/pulse except when probing the chlorine beam itself.

The ion optics configuration is a 4-lens DC slice design²² with the repeller set to 700 V and the other lenses optimized accordingly. The butenyl radical product was ionized by the 157 nm laser and accelerated up a 70 cm field-free flight tube to strike a 120 mm diameter dual microchannelplate detector coupled to a P-47 phosphor screen. The back plate was held at +1500 V, and the front plate pulsed from ground to -800 V for ~70 ns to gate detection of the central velocity slice of the mass of interest.

Images were recorded using our own NuAcq USB-2 software with an IDS UI-2230SEM camera recorded at 768 \times 768 pixels but centred to 1536 \times 1536 pixels. Recorded images were analyzed as described previously. In brief, background images obtained with the 355 nm laser off were subtracted from the laser-on image, converted to signed 16-bit data and integrated over the regions of interest after a simple density-to-flux correction.¹² Owing to intense photochemistry signal within 30° of the butene beams, reliable subtractions could not be obtained there, and data in that region is not reported.

III. RESULTS

DC sliced images of the C_4H_7 products for reactions of each of the four isomers are shown in Figure 2, with the Newton diagrams superimposed. The collision energies were 12.5, 13.3,

13.8, and 13.5 kcal·mol⁻¹ for 1-butene, trans-2-butene, cis-2-butene, and isobutene, respectively. The images are presented after background subtraction and density-to-flux correction. We emphasize that for visualization we show data with the threshold at zero, but the pixel counts are not necessarily positive after subtraction and the integrations over angle or velocity are thus reliable even in regions of substantial background.

Also shown in Figure 2 are the total center-of-mass translational energy distributions, $P(E_T)$, for each image derived from the analysis. The thick solid lines are simply smoothed fits to the integrated data, while the fine lines are the integrated raw data. There is no deconvolution of the beam velocity spreads, but these contributions are relatively small, and we would not expect to resolve any underlying features owing to the high density of states in the products.

Slice imaging methods allow for direct inversion of the experimental data, allowing one to investigate the coupling of angular and translational energy release with no assumptions about the associated dynamics.²⁴ We have found it useful to show the translational energy release separately for forward, sideways, and backscattered distributions, and these are presented in Figure 3 along with the center-of-mass angular distributions. Owing to the background interference from C_4H_8 photodissociation by the probe laser, we omit the contribution within 30° of the butene beam for the forward distributions. The angular distributions are shown as insets in the translational energy distribution plots, color-coded for the different regions to match the appropriate $P(E_T)$ segments. Another useful aspect for interpreting the translational energy distribution plots is featured in Figure 3: Rather than giving the distributions in terms of total translational energy, we plot in terms of reduced translational energy, $E_T^* = E_T/E_{coll}$. This is useful because for heavy-light-heavy systems, the acute skew angle implies that conservation of translational energy is expected.¹² This is true both for near-collinear collisions, for which the light H atom is kinematically disfavored for coupling exoergicity into product recoil, or for large impact parameter

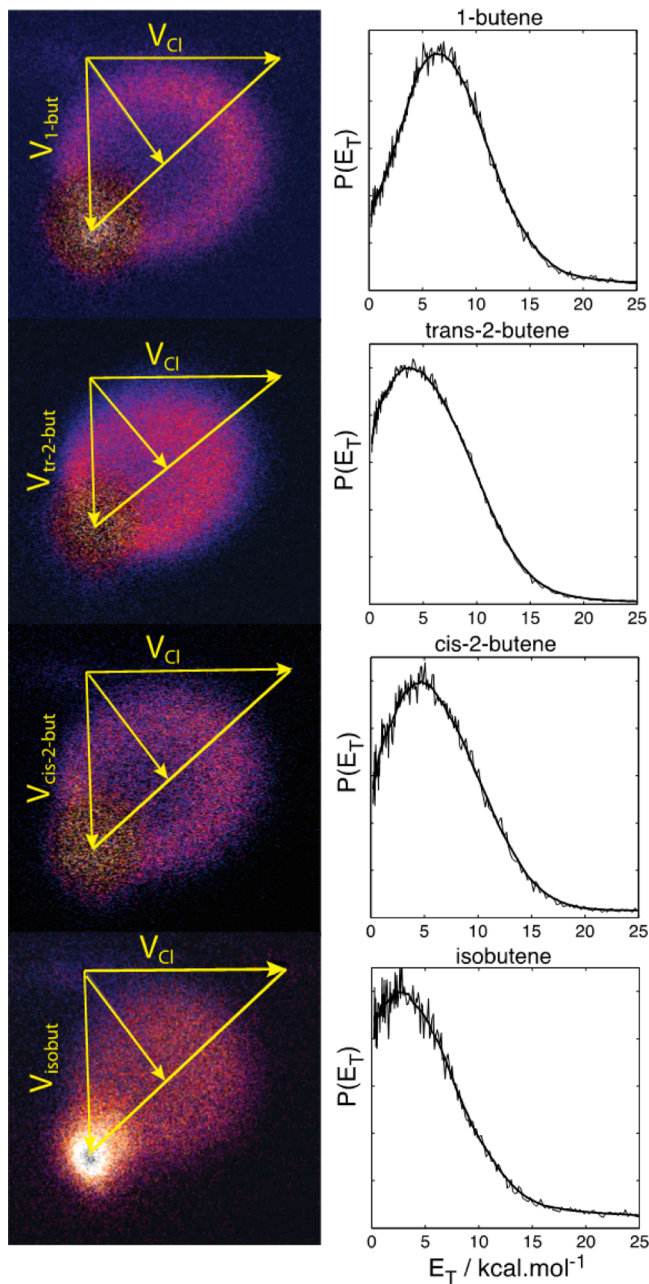


Figure 2. DC sliced images for the C_4H_7 products of reaction for the indicated target isomers with the most probable Newton diagrams superimposed (left) and global translational energy distributions obtained from the images (right).

collisions, for which the small momentum transfer also precludes product energy release appearing in translation. By plotting these distributions against E_T^* , we can see at a glance the nature of the deviation from the limiting cases.

The average translational energy release and fraction of the collision energy appearing in translation is compiled in Table 1, consistent with the translational energy distributions plotted in Figures 2 and 3. We also show the total available energy assuming abstraction at the allylic site, and the corresponding fraction of the available energy appearing in translation. Owing to the large exoergicity, this fraction is substantially smaller than the fraction of collision energy that is conserved.

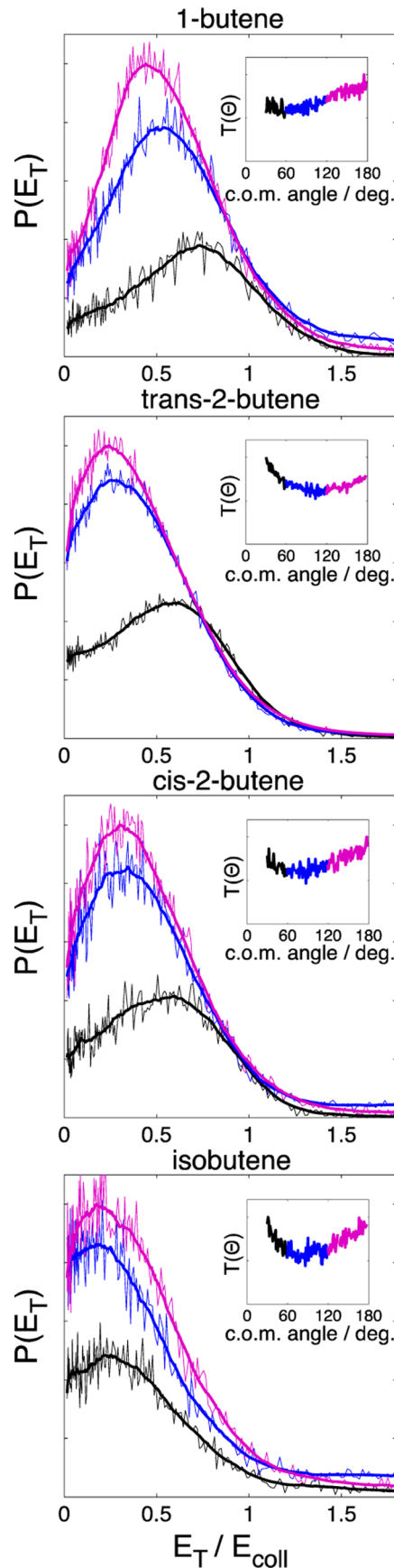


Figure 3. Reduced translational energy distributions for forward (black), sideways (blue), and backward (purple) scattered distributions, with the center-of-mass angular distributions inset in each plot.

Table 1. Collision Energies, Available Energies for Allylic H Abstractions, and Average Translational Energy Releases in $\text{kcal}\cdot\text{mol}^{-1}$; the Latter Are Given along with the Fractions f_T of Collision Energy or Maximum Available Energy for Indicated Center-of-Mass Scattering Regions

	E_{coll}	E_{avail}	total 30–180°			forward 30–60°			sideways 60–120°			backward 120–180°		
			$\langle E_T \rangle$	$f_{T(\text{coll})}$	$f_{T(\text{avail})}$									
gauche-1-but	12.5	33.3	7.7	0.61	0.23	8.4	0.67	0.25	7.7	0.61	0.23	7.0	0.56	0.21
trans-2-but	13.3	31.3	6.2	0.46	0.20	7.4	0.55	0.23	5.6	0.42	0.18	5.6	0.42	0.18
cis-2-but	13.8	32.4	6.9	0.50	0.21	7.6	0.55	0.23	6.4	0.46	0.20	6.7	0.48	0.21
isobut	13.5	30.3	6.7	0.50	0.22	7.2	0.53	0.24	6.0	0.44	0.20	6.9	0.51	0.23

IV. DISCUSSION

In the reactions of chlorine atoms with alkenes, there are several principal reactive processes that may occur^{15,25} falling into two categories: electrophilic addition to the double bond followed by collisional stabilization or HCl elimination, or direct H abstraction without access to the adduct potential well. These two broad dynamical categories may be further subdivided, depending on target isomer, into addition at the more or the less substituted carbon of the double bond, and H abstraction at an allylic site (e.g., C1 or C2 in 1-butene), an alkyl site (C3 in 1-butene), or even at a vinylic site (C4 in 1-butene). All of these processes are energetically accessible at our collision energy, but reactions of the vinylic H atoms are so unfavorable that we can safely neglect them, and the products would not be detected by the 7.9 eV probe photons in any case. For abstraction at the alkyl sites, again the vertical ionization energy exceeds our photon energy, so although this is somewhat more feasible on energetic grounds (exoergic by 2 $\text{kcal}\cdot\text{mol}^{-1}$ and probably barrierless), the product is likely not detected in our study so we will also neglect this channel. We suspect this to be a minor channel but will examine this question more closely in future work described below.

Under single-collision conditions, the addition complex cannot be stabilized so it must decompose. Typically in a radical addition to an alkene, we have anti-Markovnikov behavior, and the radical will add to the most energetically favored unsaturated carbon, which in general will be the least substituted site.¹⁵ The biggest effect here is seen in isobutene, for which the C1 site is strongly favored (see Figure 1). The addition complex may then decompose by H loss, which is endoergic by a few $\text{kcal}\cdot\text{mol}^{-1}$, by Cl elimination returning to reactants or by HCl elimination. For the latter reaction, the allylic site is strongly favored, and the large exoergicity might suggest formation of vibrationally excited HCl. In fact, substantial vibrational excitation in the HCl product has been used in kinetics studies as a marker for direct reaction, as this exoergic process would be characterized by an early transition state (TS).²⁵ The addition/elimination was assumed to give lower vibrational excitation owing to energy randomization in the long-lived adduct. On this basis, a large fraction of the direct component was inferred. This approach was developed by Setser and co-workers²⁵ and further considered by Taatjes and co-workers.¹⁵

In our previous study with C5 and C6 monoalkenes under single-collision conditions, we inferred almost exclusive reaction via addition/elimination.¹⁷ This was based on angular distributions that were nearly isotropic and translational energy distributions that peaked near zero. The highest collision energy studied in that work was 7 $\text{kcal}\cdot\text{mol}^{-1}$, however, significantly less than what we employ here. Nevertheless, here we see significant variations in the behavior with different

isomers, while in the earlier study even distinct molecules were largely indistinguishable from each other in their product distributions.

By examining the global translational energy distributions in Figure 2, we see that 1-butene peaks farthest from zero at 6–7 $\text{kcal}\cdot\text{mol}^{-1}$, the two 2-butene isomers are intermediate, peaking at 4–5 $\text{kcal}\cdot\text{mol}^{-1}$, and isobutene shows the lowest energy peak at 2–3 $\text{kcal}\cdot\text{mol}^{-1}$. If we assume that the lower translational energy peak is associated with a greater fraction of the indirect reaction, then the importance of adduct formation increases in the same order and is most important for isobutene. This is further supported by the angle-dependent translational energy distributions shown in Figure 3 along with the angular distributions. Here, a distinction between the forward scattering and the backward and sideways scattering clearly indicates a direct component to the reaction. Again, this distinction is greatest for 1-butene, intermediate for the two 2-butenes, and absent for isobutene.

These trends are also reflected in the average translational energy release summarized in Table 1 and consistent with the relative stabilities of the adducts and abstraction reactions shown in Figure 1. 1-Butene (we consider only the gauche conformer²⁶) has the shallowest well, and the most exoergic abstraction channel, suggesting that the indirect reaction would be least important for this molecule. Isobutene has both the deepest well (for addition at the C1 site) and the lowest exoergicity for abstraction. On this basis alone we would anticipate the greater role for a long-lived intermediate for isobutene, which is consistent with the translational energy distributions in Figures 2 and 3.

A crucial underlying question, and one that is implicit in the interpretation of Setser and raised by Taatjes et al., is the nature of the TS for HCl elimination from the adduct, both its height and its geometry. One would expect low vibrational excitation in the HCl product from adduct decomposition if one assumes product-like or intermediate geometry for the TS. A preliminary survey in 1-butene has failed to identify a TS for HCl elimination from the adduct.²⁷ One possible explanation for this is that the decomposition occurs primarily via a Cl atom roaming reaction.^{28,29} This picture is supported by earlier theoretical examination of H_2 addition to radicals.^{30–32} For H_2 addition to vinyl radical, electron density must be donated from the singly occupied p orbital of σ character in the radical plane to the σ_u orbital in H_2 , the most favorable interaction being in the collinear abstraction geometry. Mebel and co-workers argued that this is a general feature of H_2 addition to σ radicals, and similar arguments would apply to the reverse reactions. If we extend this picture to HCl, H_2 , and allylic radicals as well as vinyl, then we infer that the favored C–H–Cl abstraction geometry would be accessed most readily by a roaming event. In this case, the vibrational excitation in HCl for the direct and indirect reactions at the allylic site could be very similar (and

likely quite substantial). This is analogous to the H₂ vibrational excitation seen in the roaming channel and the direct component of the H + HCO reaction reported by Bowman and co-workers.³³ If most adduct decomposition occurs via roaming, then the HCl vibrational excitation may be largely uncorrelated with the lifetime of the intermediate, and low vibrational excitation may reflect reactions at alkyl sites or other aspects of the dynamics. Furthermore, the kinetic isotope effects (KIE) in these reactions^{34,35} examined by Finlayson-Pitts and co-workers will be complicated: the addition step would be characterized by an inverse KIE (the higher density-of-states in the deuterated molecule stabilizes the adduct compared to the undeuterated molecule), while the roaming-abstraction step would show a normal KIE owing to the difference in zero-point energies. It is not clear how these opposing effects would manifest themselves in the observed KIE, but it is an interesting subject for investigation.

V. CONCLUSIONS

We have studied the reactions of chlorine atoms with a variety of butene isomers, namely, 1-butene, *trans*-2-butene, *cis*-2-butene, and isobutene, using DC sliced imaging in a crossed-beam apparatus at collision energies of \sim 13 kcal·mol⁻¹. The reactions showed distinct behavior for the various isomers that is interpreted as largely reflecting the relative importance of addition/elimination (complex formation) vs direct reaction. The VUV probe at 157 nm is sensitive only to reaction at the allylic site, which is likely to be the dominant reaction site for all isomers considered. A key question is raised concerning the decomposition of the complex and whether it occurs via a roaming radical mechanism. If this is the case, then the HCl product vibrational distributions may not be a sensitive measure of direct vs indirect reaction. We plan detailed energy-dependent crossed-beam studies and more extensive theoretical investigations to address these questions.

AUTHOR INFORMATION

Corresponding Author

*E-mail: asuits@chem.wayne.edu.

Notes

The authors declare no competing financial interest.

ACKNOWLEDGMENTS

This work was supported by the Director, Office of Science, Office of Basic Energy Sciences, Division of Chemical Science, Geoscience and Bioscience, of the US Department of Energy under contract number DE-FG02-04ER15593. We thank Prof. A. Mebel for valuable discussions.

REFERENCES

- (1) Murray, C.; Orr-Ewing, A. J. The Dynamics of Chlorine-Atom Reactions with Polyatomic Organic Molecules. *Int. Rev. Phys. Chem.* **2004**, *23*, 435.
- (2) Yen, Y. F.; Wang, Z. R.; Xue, B.; Koplitz, B. Site Propensities for HCl and DCI Formation in the Reaction of Cl with Selectively-Deuterated Propanes. *J. Phys. Chem.* **1994**, *98*, 4.
- (3) Varley, D. F.; Dagdigian, P. J. Product State Distributions and Angular Differential Cross-Sections from Photoinitiated Reactions of Chlorine Atoms with Small Hydrocarbons. *J. Phys. Chem.* **1995**, *99*, 9843.
- (4) Varley, D. F.; Dagdigian, P. J. Comparison of the Dynamics of Abstraction of Primacy vs. Secondary Hydrogens in the Cl + CD₃CH₂CD₃ Reaction. *Chem. Phys. Lett.* **1996**, *255*, 393.
- (5) Varley, D. F.; Dagdigian, P. J. Product State Resolved Study of the Cl + (CH₃)₃CD Reaction: Comparison of the Dynamics of Abstraction of Primary versus Tertiary Hydrogens. *J. Phys. Chem.* **1996**, *100*, 4365.
- (6) Simpson, W. R.; Rakitzis, T. P.; Kandel, S. A.; Orr-Ewing, A. J.; Zare, R. N. Reaction of Cl with vibrationally excited CH₄ and CHD₃: State-to-State Differential Cross-Sections and Steric Effects for the HCl Product. *J. Chem. Phys.* **1995**, *103*, 7313.
- (7) Kandel, S. A.; Rakitzis, T. P.; Lev-On, T.; Zare, R. N. Dynamical Effects of Reagent Vibrational Excitation in the Cl + C₂H₆($\nu_5 = 1$) \rightarrow HCl + C₂H₅ Reaction. *Chem. Phys. Lett.* **1997**, *265*, 121.
- (8) Orr-Ewing, A. J.; Simpson, W. R.; Rakitzis, T. P.; Kandel, S. A.; Zare, R. N. Scattering-Angle Resolved Product Rotational Alignment for the Reaction of Cl with vibrationally excited Methane. *J. Chem. Phys.* **1997**, *106*, 5961.
- (9) Shafer, N. E.; Orr-Ewing, A. J.; Simpson, W. R.; Xu, H.; Zare, R. N. State-to-State Differential Cross-Sections from Photoinitiated Bulb Reactions. *Chem. Phys. Lett.* **1993**, *212*, 155.
- (10) Murray, C.; Pearce, J. K.; Rudic, S.; Retail, B.; Orr-Ewing, A. J. Stereodynamics of Chlorine Atom Reactions with Organic Molecules. *J. Phys. Chem. A* **2005**, *109*, 11093.
- (11) Blank, D. A.; Hemmi, N.; Suits, A. G.; Lee, Y. T. A Crossed Molecular Beam Investigation of the Reaction Cl + Propane \rightarrow HCl + C₃H₇ Using VUV Synchrotron Radiation as a Product Probe. *Chem. Phys.* **1998**, *231*, 261.
- (12) Estillore, A. D.; Visger, L. M.; Suits, A. G. Crossed-Beam DC Slice Imaging of Chlorine Atom Reactions with Pentane Isomers. *J. Chem. Phys.* **2010**, *132*, 164313.
- (13) Li, W.; Huang, C. S.; Patel, M.; Wilson, D.; Suits, A. State-Resolved Reactive Scattering by Slice Imaging: A New View of the Cl + C₂H₆ Reaction. *J. Chem. Phys.* **2006**, *124*, 11102.
- (14) Bass, M. J.; Brouard, M.; Cireasa, R.; Clark, A. P.; Vallance, C. Imaging Photon-Initiated Reactions: A Study of the Cl(²P_{3/2}) + CH₄ \rightarrow HCl + CH₃ Reaction. *J. Chem. Phys.* **2005**, *123*, 94301.
- (15) Taatjes, C. A. Time-Resolved Infrared Absorption Measurements of Product Formation in Cl Atom Reactions with Alkenes and Alkynes. *Int. Rev. Phys. Chem.* **1999**, *18*, 419.
- (16) Tyndall, G. S.; Orlando, J. J.; Wallington, T. J.; Dill, M.; Kaiser, E. W. Kinetics and Mechanisms of the Reactions of Chlorine Atoms with Ethane, Propane, and *n*-Butane. *Int. J. Chem. Kinet.* **1997**, *29*, 43.
- (17) Estillore, A. D.; Visger, L. M.; Suits, A. G. Imaging the Dynamics of Chlorine Atom Reactions with Alkenes. *J. Chem. Phys.* **2010**, *133*, 074306.
- (18) Montgomery, J. A.; Frisch, M. J.; Ochterski, J. W.; Petersson, G. A. A Complete Basis Set Model Chemistry. VII. Use of the Minimum Population Localization Method. *J. Chem. Phys.* **2000**, *112*, 6532.
- (19) Frisch, M. J.; Trucks, G. W.; Schlegel, H. B.; Scuseria, G. E.; Robb, M. A.; Cheeseman, J. R.; Scalmani, G.; Barone, V.; Mennucci, B.; Petersson, G. A.; et al. *Gaussian 09*, revision A.02; Gaussian, Inc.: Wallingford, CT, 2009.
- (20) Ahmed, M.; Peterka, D. S.; Suits, A. G. H Abstraction Dynamics by Crossed-Beam Velocity Map Imaging: Cl + CH₃OH \rightarrow CH₂OH + HCl. *Chem. Phys. Lett.* **2000**, *317*, 264.
- (21) Ahmed, M.; Blunt, D.; Chen, D.; Suits, A. G. UV Photo-dissociation of Oxalyl Chloride Yields Four Fragments from One Photon Absorption. *J. Chem. Phys.* **1997**, *106*, 7617.
- (22) Townsend, D.; Miniti, M. P.; Suits, A. G. Direct Current Slice Imaging. *Rev. Sci. Instrum.* **2003**, *74*, 2530.
- (23) Li, W.; Chambreau, S. D.; Lahankar, S. A.; Suits, A. G. Megapixel Ion Imaging with Standard Video. *Rev. Sci. Instrum.* **2005**, *76*, 63106.
- (24) Townsend, D.; Li, W.; Lee, S. K.; Gross, R. L.; Suits, A. G. Universal and State-Resolved Imaging of Chemical Dynamics. *J. Phys. Chem. A* **2005**, *109*, 8661.
- (25) Arunan, E.; Rengarajan, R.; Setser, D. W. Infrared Chemiluminescence Studies of the Reactions of H Atoms with CCl₃, CF₂Cl, and CH₂CH₂Cl Radicals at 300 and 475 K: Recombination-Elimination vs. Abstraction Mechanisms. *Can. J. Chem.* **1994**, *72*, 568.

- (26) Kunitski, M.; Knippenberg, S.; Dreuw, A.; Brutschy, B. The Conformational Stability of Gaseous 1-Butene Studied by Femtosecond Nonlinear Spectroscopy and ab Initio Calculations. *Vib. Spectrosc.* **2011**, *56*, 13.
- (27) Mebel, A. Private Communication.
- (28) Bowman, J. M.; Shepler, B. C. Roaming Radicals. *Annu. Rev. Phys. Chem.* **2011**, *62*, 531.
- (29) Suits, A. G. Roaming Atoms and Radicals: a New Mechanism in Molecular Dissociation. *Acc. Chem. Res.* **2008**, *41*, 873.
- (30) Kim, G.-S.; Nguyen, T. L.; Mebel, A. M.; Lin, S. H.; Nguyen, M. T. Ab Initio/RRKM Study of the Potential Energy Surface of Triplet Ethylene and Product Branching Ratios of the C(³P) + CH₄ Reaction. *J. Phys. Chem. A* **2003**, *107*, 1788.
- (31) Mebel, A.; Lin, M.; Yu, T.; Morokuma, K. Theoretical Study of Potential Energy Surface and Thermal Rate Constants for the C₆H₅ + H₂ and C₆H₆ + H Reactions. *J. Phys. Chem. A* **1997**, *101*, 3189.
- (32) Mebel, A. M.; Morokuma, K.; Lin, M. Ab Initio Molecular Orbital Study of Potential Energy Surface for the Reaction of C₂H₃ with H₂ and Related Reactions. *J. Chem. Phys.* **1995**, *103*, 3440.
- (33) Christoffel, K. M.; Bowman, J. M. Three Reaction Pathways in the H + HCO → H₂ + CO Reaction. *J. Phys. Chem. A* **2009**, *113*, 4138.
- (34) Stutz, J.; Ezell, M.; Ezell, A.; Finlayson-Pitts, B. Rate Constants and Kinetic Isotope Effects in the Reactions of Atomic Chlorine with *n*-Butane and Simple Alkenes at Room Temperature. *J. Phys. Chem. A* **1998**, *102*, 8510.
- (35) Stutz, J.; Ezell, M.; Finlayson-Pitts, B. Inverse Kinetic Isotope Effect in the Reaction of Atomic Chlorine with C₂H₄ and C₂D₄. *J. Phys. Chem. A* **1997**, *101*, 9187.